Citation： Jian-Xin Lu, Peiliang Shen, Haibing Zheng, Baojian Zhan, Hafiz Asad Ali, Pingping He, Chi Sun Poon*, Synergetic recycling of waste glass and recycled aggregates in cement mortars: Physical, durability and microstructure performance, Cement and Concrete Composites 113 (2020) 103632. https://doi.org/10.1016/j.cemconcomp.2020.103632

Synergetic recycling of waste glass and recycled aggregates in cement mortars: Physical, durability and microstructure performance

Jian-Xin Lu, Peiliang Shen, Haibing Zheng, Baojian Zhan, Hafiz Asad Ali, Pingping He, Chi Sun Poon*

The Hong Kong Polytechnic University, Department of Civil and Environmental Engineering, Hung Hom, Kowloon, Hong Kong

* Corresponding author: cecspoon@polyu.edu.hk (C.S. Poon)

Abstract

The generation of large quantities of waste glass and construction waste has increasingly become an environmental burden in city governments. This study investigated the joint utilization of recycled glass cullet (RGC) and recycled fine aggregates (RFA) in cement mortars. The mechanical, durability and microstructure properties of the cement mortars were evaluated. The experimental results showed that the synergetic reuse of RGC and RFA in cement mortars was feasible both from mechanical and durability points of view. The replacement of RGC by RFA was beneficial to enhancing the compressive strength of cement mortars due to the improvement of the interfacial transition zone and microhardness of the paste matrix, and the refinement of the pore structures. Encouragingly, the combined use of RGC and RFA in cement mortars could exhibit low drying shrinkage and alkali-silica reaction expansion. In particular, the acid resistance of the cement mortars was improved effectively when the RGC was used in conjunction with RFA as 100% fine aggregates in the mortars.

Keywords: Waste glass; Recycled aggregates; Cement mortar; Durability; Interfacial transition zone (ITZ); Pore structure

1. Introduction

1.1 Scarcity of river sand

River sand (RS) is regarded as the optimal fine aggregate for the production of concrete due to its relatively round grain shape and good soundness. In recent decades, driven by the robust development of infrastructure and real estates, huge amounts of RS have been rampantly mined from rivers and lakes. The excessive exploitation of RS has considerable impacts on the water availability, navigation safety and ecological systems. Fig. 1 shows that intensive sand mining has dramatically changed the northern branch of China's largest freshwater lake within 18 years [1]. As shown, the sand dredging has eroded the riverbed and adversely changed the topography and hydrological characteristics. The frenzied extraction of sand was reported to drain the lake quickly and thus increase the drought risk [2]. Furthermore, intensive sand extraction aggravates the lake recession crisis by means of depredating the wetlands, reducing the water level, increasing turbidity and sediment concentrations, etc. [3].

Fig. 1 Intensive sand mining at Poyang Lake of China's largest freshwater lake [1]

The case of Poyang Lake is only a miniature of other fresh-water lakes in the world, and it can be anticipated that many lakes and rivers are facing the same deteriorating crisis. Given the damages caused by sand mining threaten the ecological development of local areas, many countries have limited the widespread sand exploitation. For instance, the sand dredging in the mainstream of Yangtze River (the longest river in Asia) has been prohibited by China government [4] as it has led to the demise of unique species, such as the river dolphin and finless porpoise [5].

On the other hand, the demand on RS for urbanization infrastructure is still rising massively in some developing countries and inevitably incurring price soar [6]. Therefore, the ban of sand mining on account of preserving the environment has brought about demands outstripped the supplies. For the situation of sand scarcity and high cost, it is essential to seek alternative resources for satisfying the increasing demand of fine aggregates for the construction industry.

1.2 Waste glass and recycled aggregates

In Hong Kong, due to the huge consumption of bottled beverages, a vast number of waste glass containers is generated. Based on the government statistics, the daily average of waste glass generation was about 300 tonnes over the past two decades [7]. However, the average recovery rate of waste glass during this period was less than 10% as no glass remanufacturing industry is available locally [8]. Therefore, the fate of waste glass is mostly disposed of at landfills rather than remaking new bottles.

In order to relieve the increasing burden on the landfills and pave a sustainable way for construction development, utilization of the recycled glass cullet (RGC) as aggregates in cement mortars and concrete has been widely explored [9, 10]. Since the glass material possesses high hardness and low permeability, a recent study indicated that the use of RGC had little adverse influence on the mechanical properties of concrete [11]. Moreover, the workability of cement mortar/concrete was usually improved by using RGC because of the non-hydroscopic nature of glass [12, 13]. In terms of durability performance, the inclusion of RGC into concrete could increase abilities to resist chloride ion penetration, sulfate attack and drying shrinkage [14, 15]. Especially, in engineered cementitious composites, the self-healing capability of matrix could be enhanced by incorporating recycled glass materials [16-18]. However, since most of the beverage glass is produced based on the soda-lime-silica ternary system, which contains alkaline earth oxides in combination with silica and alkali oxides, the potential deleterious alkali-silica-reaction (ASR) issue would be triggered. To address this problem, supplementary cementitious materials (SCMs), steel fiber and lithium nitrate were proven to be effective in controlling the ASR expansion [19-21]. Therefore, based on the previous investigations, the recycling of RGC as a replacement of fine aggregates may be a promising approach for producing cement-based materials.

Apart from the waste glass, construction & demolition (C&D) waste is another major component in the solid waste stream. The most common constitute of C&D waste is waste concrete. To save waste management costs and promote sustainable building products, reusing the C&D waste in the construction industry attracts significant interests [22-29]. When the C&D waste was crushed into small particles (i.e. recycled aggregates, RA), it was feasible to be employed as fine or coarse aggregates for the production of concrete or mortar [30-33]. However, most investigations focused on the use of recycled coarse aggregate in construction industry because the recycled fine aggregate (RFA) exhibited a much higher water absorption [34], which would give rise to serious loss of workability [35, 36] and large increase of shrinkage [37, 38]. Hence, compared to many guidance information on reusing recycled coarse aggregate [39], no standard has been developed to direct how to reuse RFA. Thereby, some researchers explored several treatment techniques to improve the quality of RFA, including carbonation [40], chemical and water pre-soaking [41, 42], microbial carbonate precipitation [43], surface coating [44], physical treatment and sulfuric acid washing [45, 46], chemico-thermal treatment [47], etc.. Nonetheless, these techniques usually consume large amounts of energy, supplementary materials and induce excessive costs.

For the RFA, its high water absorptivity would cause increased water demand for workability and higher drying shrinkage. On the other hand, the negligible water absorption of RGC with rich amorphous silica would lead to bleeding and ASR expansion. Therefore, by means of these two waste materials with different characteristics, this study attempts to explore the synergetic use of RGC and RFA as a replacement of natural fine aggregate for producing cement mortars. Previously, most studies paid attention to the use of RGC or RFA respectively in cement mortar and concrete. There is a lack of information on the combined reuse of glass materials and RA in the cement mortar/concrete. Nassar and Soroushian [48] found that the incorporation of RA reduced the resistance of concrete to chloride ion permeation, freeze–thaw and ASR expansion, while the joint inclusion of glass powder and RA in the concrete could counteract the adverse effect induced by RA and further improve those durability properties of concrete as compared to the control concrete. Moreover, Letelier et al. [49] found that the simultaneous incorporation of RA as fine aggregates and glass powder as a partial cement could obtain comparable mechanical properties in comparison with the control mortar at 90 days. For concurrent use of RA and glass

aggregates in self-compacting concrete, the study of Arabi et al. [50] showed that the compressive strength of concrete decreased with the increased replacement of RA by glass aggregates, while the larger quantities of glass aggregates would cause segregation risk.

1.3 Research significance

In Hong Kong, the increasing amounts of solid wastes (e.g. glass and construction wastes) encroaching lands has caused serious social and environmental problems due to the scarce sites for living. How to turn these wastes into resources is of great significance in such a small territory. Huge consumption of natural aggregates in the construction industry provides an attractive outlet for recycling these waste aggregates. Since the RGC and RFA with contrasting characteristics in physical properties and chemical structures (the RGC has smooth surface, amorphous structure, negligible water absorption, while the RFA has rough surface, crystalline structure, high water absorption) would usually have quite different influences on the properties of cement-based materials, hence, this study intends to synergistically use RGC in conjunction with RFA based on their respective physicochemical characteristics in cement mortars to achieve complementary advantage and mutual benefit. The objective of this investigation is to jointly use these two waste aggregates in lieu of the natural fine aggregates to develop a good functional and durable construction product. The intended use of this eco-cement mortar will be a plastering or rendering mortar for buildings. It is expected that combined recycling of RGC and RFA in construction industry will not only mitigate the landfills burden but also reduce the consumption and dependence of natural RS. Up to now, far too little attention has been paid to use RGC and RFA simultaneously as fine aggregates in cement mortars. Hence, the relevant hardened properties, durability and microstructure characteristics of cement mortars prepared with RGC and RFA were comprehensively investigated in this study.

2. Experimental design

2.1 Materials

The binders used to produce the cement mortars were Ordinary Portland cement and ground granulated blast-furnace slag (GGBS). The OPC was ASTM type I (52.5 class) and was produced locally by Green Island Cement. The GGBS was a byproduct of steel

160 production, which was sourced from Mainland China. The GGBS was introduced into
161 the cement mortars as a SCM. Fig. 2(a) shows the particle size distributions of OPC
162 and GGBS. The chemical compositions and mean particle sizes of cementitious
163 materials (OPC and GGBS) are listed in Table 1.
164
165 Table 1 Chemical compositions and physical properties of binders (OPC and GGBS)
166 and aggregates (RGC, RFA and RS)

Chemical composition, %	OPC	GGBS	RGC	RFA	RS
SiO_2	20.33	34.78	69.0	64.8	90.8
Al_2O_3	5.21	14.22	2.62	19.5	4.99
Fe_2O_3	3.13	0.72	1.42	2.88	0.84
CaO	64.00	38.38	10.5	2.97	0.68
Na_2O	/	/	13.5	2.26	/
MgO	1.62	7.32	1.35	0.93	0.26
K_2O	0.63	0.77	0.79	5.87	2.08
SO_3	4.17	3.12	0.13	0.14	0.09
TiO_2	0.27	0.71	/	0.26	0.09
P_2O_5	0.20	/	0.12	0.20	0.10
Specific gravity	3.15	2.56	2.52	2.61	2.68
Mean diameter (μm)	29.7	12.9	/	/	/

167
168 The fine aggregates used in this study included RGC, RFA and natural RS. The RGC
169 used was sourced from the recycling of waste soda-lime-silica glass, which was
170 obtained from a glass recycling facility after crushing post-consumer beverage bottles.
171 The RFA was collected from a C&D recycling facility in Hong Kong. Table 1 lists the
172 oxide compositions of three aggregates by mass determined by X-ray fluorescence
173 (XRF) spectrometer (Rigaku, Supermini200). The major oxides were SiO_2, CaO and
174 Na_2O in the RGC, and SiO_2, Al_2O_3, and K_2O in the RFA, RS mainly consisted of SiO_2.
175 The gradation curves of RGC, RFA and RS are presented in Fig. 2(b), which shows that
176 all the fine aggregates used were within the boundaries for fine aggregates as stated in
177 the BS standard. However, the particle size distribution of RFA was more biased to the
178 lower boundary while the particle size distribution of RS was nearer to the upper sieve
179 size. Also, the fineness modulus of the RGC, RFA and RS were 3.0, 3.3 and 2.3
180 respectively (Table 2), which indicates the particle size of RFA was the largest and that
181 of RS was the smallest.

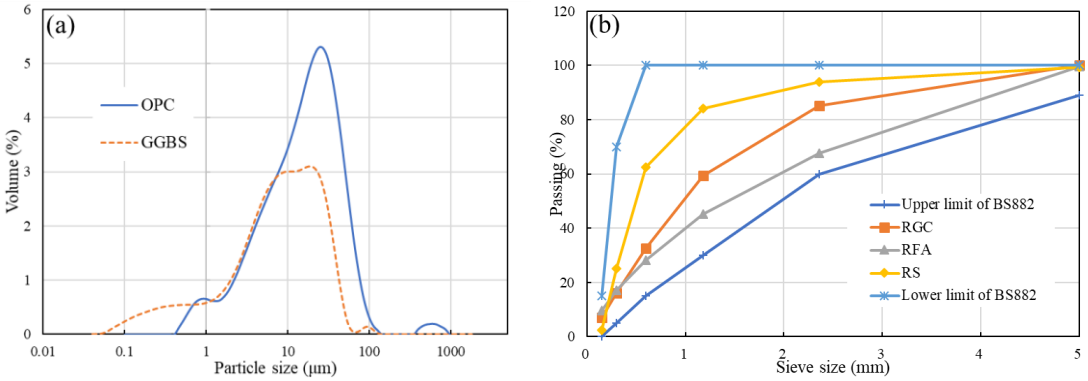

Fig. 2 Particle size distributions of OPC and GGBS (a),
Gradation curves of fine aggregates (b)

182

183 The appearances of RFA and RGC are also shown in Fig. 3. It should be noted that the
184 batch of RFA used in this study was mainly crushed from recycled rock derived from
185 excavation from construction sites, thereby it contained a certain amount of clay. Also,
186 it was found that the RGC contained some papers resulting from the crushed label
187 attached on the glass bottles. Before use, the RFA, RGC and RS were oven dried at
188 105 °C for 24 hours to remove moisture. The physical properties of the aggregates are
189 presented in Table 2. It can be found that the RGC had a negligible water absorption by
190 reason of its hydrophobic nature, while the RFA had a much higher water absorption
191 due to the rough texture and the presence of a certain quantity of fine particles, which
192 were mostly silty soil and granite dust.

193

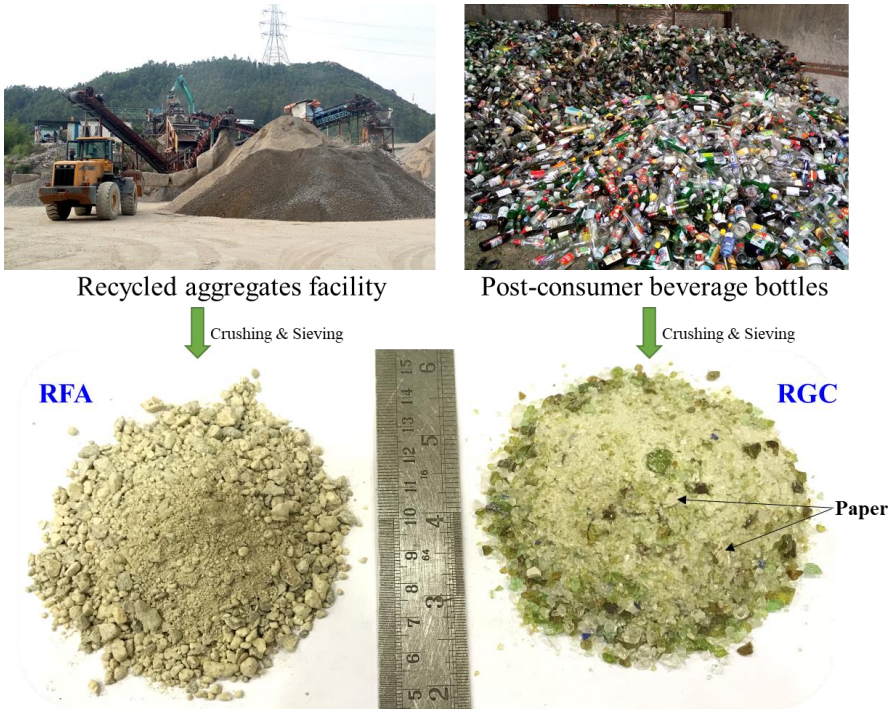

Fig. 3 Production and appearances of RFA and RGC

194

195 Table 2 Physical properties of RGC, RFA and RS

Properties	RGC	RFA	RS
Fineness modulus	3.0	3.3	2.3
Water absorption (%)	0.33	3.86	0.66
Density (kg/m^3)	2.52	2.61	2.68
Fines content (%, ＜75 μm)	4.32	16.76	1.38

196

197 **2.2 Mineralogy and thermal stability of aggregates**

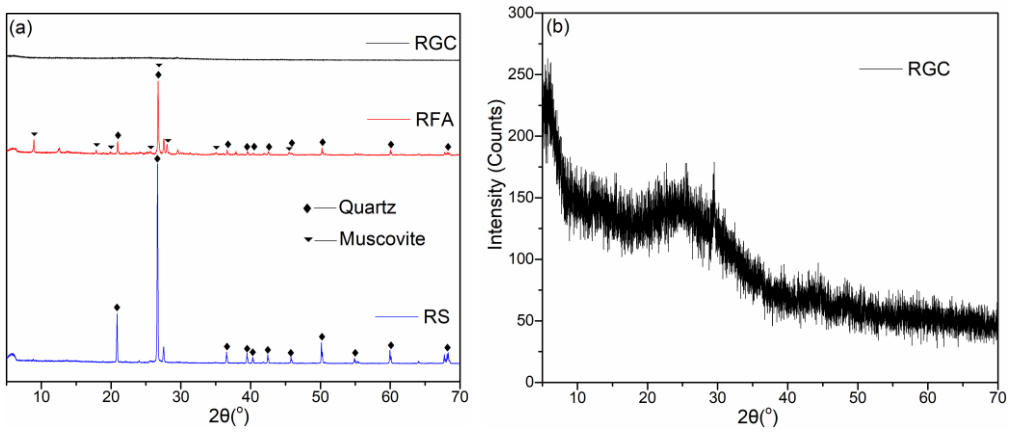

Fig. 4 XRD patterns of RFA, RGC and RS (a), magnification of RGC (b)

198

The mineralogy of RFA, RGC and RS was determined by X-ray diffraction analysis (XRD) with the following operating parameters: Cu Kα radiation, 45 kV, 200 mA power generator. An angular range of 5–70° 2θ was measured with a scan speed of 5° per minute. Powdered samples (<75 μm) were prepared for testing. Fig. 4 presents the XRD patterns of three different aggregates. The RS shows a strong crystalline phase of quartz (SiO_2). Compared to the RS, the intensity of quartz was weaker in the RFA, but the muscovite ($(KF)_2(Al_2O_3)_3(SiO_2)_6(H_2O)$) mineral was found in the RFA. This was the reason why the RFA contained a relatively higher amount of alumina (see Table 1). The presence of quartz and muscovite suggests that the granite was the primary component in the RFA as the quartz and muscovite (the most common mica) usually intergrowth in granites [51]. It can be seen that the XRD pattern of RGC had no diffraction peaks identifiable to any crystalline phases (Fig. 4a). Only a huge hump was detected in Fig. 4b, which indicates that the RGC was a completely amorphous material. Hence, the fine glass particles in the RGC shown in Table 2 would possess some pozzolanic reactivity [52].

The thermogravimetric (TG) analysis coupling with differential thermal analysis (DTA) were conducted to evaluate the thermal stability of aggregates by using a Rigaku instrument (Thermo Plus Evo2 8121). The temperature rose from 30 °C to 1000 °C at a heating rate of 10 °C per minute in air. Approximate 10 mg powdered sample (<75 μm) was used for the measurement. Fig. 5 shows the TG and DTA curves of RFA, RGC and RS. It was clearly seen that RS had negligible mass loss exposed to high temperature. However, an exothermic peak present at 568 °C in the DTA curve indicates the α-quartz undergone a change in crystal structure to β-quartz. This transition was accompanied by a thermal expansion [53]. The structural transformation of quartz was also found in the RFA at 570 °C. Since the quartz content in the RS was much higher than that in the RFA based on the composition and mineralogy results, it was expected that the crystal inversion of quartz was more severe for the RS aggregate. The RGC did not exhibit the crystalline transition due to its amorphous structure. However, an amorphous rigid state of glass will turn into a viscous liquid at the glass transition temperature. The DTA trace showed a well-defined glass transition, which located at nearly 640 °C. A relatively higher mass loss was observed at the low temperature as the RGC contained some impurities from beverage bottles, such as paper and plastic. The mass loss of the RFA was interpreted to the decomposition of muscovite [54].

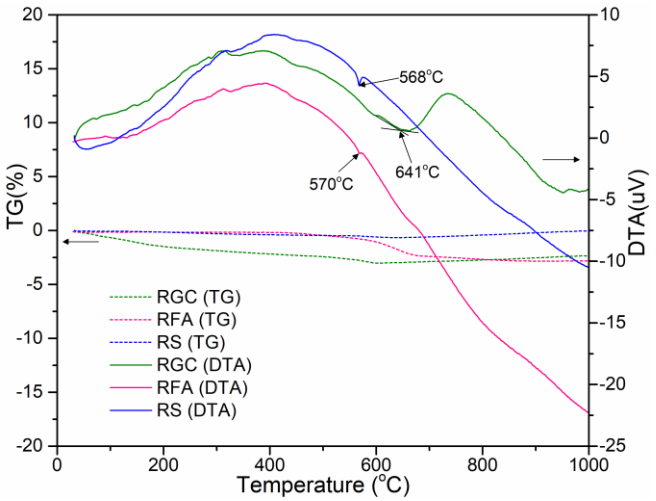

Fig. 5 TG and DTA curves of RGC, RFA and RS

2.3 Mix proportion and preparation

Six mix proportions of cement mortars were designed for evaluating the feasibility of using RGC and RFA simultaneously as fine aggregates. The water to binder (*w*/*b*) ratio was set at 0.5 and the fine aggregates to binder ratio was fixed at 2.0. Considering the RFA had high water absorption while RGC had negligible water absorption and rich in amorphous silica, the mix proportions were originally designed to explore how much of RGC can counteract the increased drying shrinkage from RFA and how much of RFA can mitigate the ASR expansion from RGC. Based on this concept, the RFA was used gradually as 0%, 25%, 50%, 75% and 100% by weight replacements of RGC (marked as 100G, 75G25R, 50G50R, 25G75R and 100R). In addition, the mortar prepared with 100% RS was also produced in comparison with the mortars prepared with the recycled aggregates.

Considering the use of waste glass as aggregates may induce ASR, 20% of OPC was replaced by a common SCM (i.e. GGBS), which was indicated in our previous study that the incorporation of 20% GGBS could successfully suppress the ASR expansion in glass mortars [19]. A certain amount of polycarboxylate superplasticizer (SP) was used to achieve a desired workability with a flow value about 235 ± 5 mm (based on the BS EN1015 [55]). The dosage of SP was based on the percentage of the total binder. The design of the mortars with a high flowability is to cope with the workability loss due to off-site transportation of ready-mixed mortars. The mix proportions of the mixes are listed in Table 3.

Table 3 Mix proportions of cement mortars (kg/m^3)

Mix	OPC	GGBS	RGC	RFA	RS	Water	SP
100G	503	126	1257	0	0	314	1.9 (0.3%)
75G25R	503	126	943	314	0	314	5.0 (0.6%)
50G50R	503	126	629	629	0	314	6.5 (1.0%)
25G75R	503	126	314	943	0	314	9.2 (1.5%)
100R	503	126	0	1257	0	314	12.6 (2.0%)
100S	503	126	0	0	1257	314	3.8 (0.6%)

For the preparation of the cement mortars, the binders and the aggregates were weighed and blended homogeneously in a mortar mixer. Then, water with an appropriate amount of SP was added to the dry materials and the mixture was further mixed to form a uniform mixture with the specified flowability. Subsequently, the fresh mixtures were fabricated in steel moulds with size of 50×50×50 mm^3. The moulds were covered with plastic sheets to avoid moisture evaporation. After 24 hours, the cement mortars were demoulded and cured in the water tank with 25 °C until testing.

2.4 Properties of cement mortars

2.4.1 Density and water absorption

The dry bulk density of cement mortars was determined in accordance with BS EN 1015-10 for hardened mortars [56]. The volume of each specimen (50×50×50 mm^3) was tested by the water displacement method based on BS EN 12390-7 [57]. After taking out of specimens from water curing tank (28 days of curing), the mass of specimens immersed in water (M_{Water}) was determined by placing in a stirrup. Then, the specimens were removed from the stirrup and the surplus water on the surfaces was wiped out using a damp cloth. Recording the mass of the specimens under saturated-surface-dry (SSD) condition in air (M_{SSD}). Assuming the density of water at ambient temperature is 1 g/cm^3. The volume of specimens can be obtained as the subtraction of M_{SSD} and M_{Water}. Afterward, the specimens were transferred to a ventilated oven for drying at a temperature of 105 °C until reaching mass constant (M_{Dry}). Hence, the dry bulk density (ρ) of each mortar specimen can be calculated as the ratio of the M_{Dry} to the volume (M_{SSD}–M_{Water}) as the following equation. The water absorption (w) of cement mortars could also be calculated using the formula.

$$\rho = \frac{M_{Dry}}{M_{SSD} - M_{Water}}$$

$$w = \frac{M_{SSD} - M_{Dry}}{M_{Dry}} * 100\%$$

where:

ρ stands for the dry bulk density of the cement mortars (g/cm^3);

w represents the water absorption of the cement mortars (%);

M_{SSD} means the mass of the saturated specimen under SSD condition (g);

M_{Water} represents the mass of the saturated specimen immersing in water (g);

M_{Dry} means the mass of oven-dried specimen in air (g).

2.4.2 Compressive strength

The compressive strength of cement mortars with size of 50×50×50 mm^3 was measured by a compaction machine (3000 kN). The loading rate was set to 0.6 MPa/s. Three specimens were determined to obtain an average value of strength.

2.4.3 Drying shrinkage

The dry shrinkage test for the cement mortars was carried out according to BS ISO 1920-8 [58]. Cement mortars were cast into steel moulds with dimension of 25W×25H×285L mm^3 prisms. After 24 hours, the cement mortars were demoulded and the initial lengths of the prism specimens were measured. Then, the specimens were transferred to a drying chamber at 25 °C and 50% relative humidity. Three specimens of each batch were taken out from chamber for length measurement at 1st, 4th, 7th, 14th, 28th, 45th day.

2.4.4 ASR

Although the GGBS was already used as a SCM to suppress the potential ASR expansion, the ASR test was also conducted to ascertain that no deleterious expansion would occur. The test method was carried out in accordance with ASTM C1260 [59]. The size of specimens was the same with the shrinkage experiment. After demolding at 24 hours after casting, the specimens were immersed into a water bath (80 °C) for another 24 hours, and then initial lengths of the bars were recorded by using a length comparator. Immediately afterwards, the specimens were transferred into a NaOH solution (1 N, 80 °C). At the testing time (1st, 4th, 7th, 14th, 21st, 28th day), the

specimen bars were removed from the alkali solution and the length changes were measured within 15s.

2.4.5 High temperature resistance

High temperature exposure was conducted to determine the resistance of the cement mortars against fire. After the density and water absorption measurements, the over-dried specimens were transferred into an electric furnace. Subsequently, the temperature was increased to 800 °C at a rate of 5 °C /min and the maximum temperature kept for 2 hours. After cooling naturally to room temperature, the residual compressive strength was tested. Three specimens for each batch were tested to obtain an average value. Based on the compressive strength values of the specimens with and without exposure to the high temperature, the strength loss (*SL*) of the cement mortars can be calculated by the following equation.

$$SL = (1 - \frac{S_r}{S_i}) \times 100\%$$

where:

S_r is the residual compressive strength of sample after subjecting to 800 °C;

S_i is the initial compressive strength of sample without subjecting to 800 °C.

2.4.6 Acid resistance

The chemical resistance of the cement mortars was also carried out according to ASTM C 267 [60]. Three cube mortars (50×50×50 mm^3) at SSD condition were used for consecutive testing. The initial mass of each specimen was weighted and then the specimens were soaked in a 3% sulfuric acid solution. The acid concentration of solution was maintained by renewing weekly. The mass measurement was performed for the corroded specimens at SSD condition in one-week intervals. The cumulative mass loss (*ML*) of each specimen can be calculated by the following formula:

$$ML = \frac{M_t - M_i}{M_i} \times 100\%$$

where:

M_t is the mass of specimen at immersion time t;

M_i is the initial mass of specimen without immersion in sulfuric acid.

2.4.7 Microstructure analysis

A tungsten thermionic emission scanning electron microscope (SEM, JEOL Model

JSM-6490) was employed to observe the morphological changes of the cement mortar fractured surfaces, especially the interfacial transition zones (ITZ) between the aggregates and the cement paste. After testing the strength of the cement mortars at the curing age of 28 days, the samples were broken into pieces and then immersed into ethanol for two weeks to stop further hydration. Afterwards, they were transferred to a vacuum chamber at 60 °C for drying for another two weeks. SEM observation was carried out on the gold-coated fractured surfaces. The testing was done at a high vacuum condition with a voltage of 20 kV and current of 70-90 mA. The working distance of the equipment was set at 10 mm.

A HVX1000A Vickers microhardness equipment was employed to determine the microhardness of the interfacial zone and the cement paste of the mortar specimens. After 28 days curing, the cube mortars were cut by a diamond saw to small slices, which were then dried in a freeze-dryer for 48 hours. Afterwards, the specimens were embedded into a low viscosity epoxy resin under vacuum condition for 24 hours, followed by finely grinding and polishing on the cutting surface. The measurement was conducted from the surface of the aggregates and extended toward the paste matrix at an interval of 30 μm. At least five measurements were taken to obtain an average value.

The pore structure of cement mortars was determined by mercury intrusion porosimetry (MIP, Micromeritics AutoPore IV 9500 Series). The specimens used for MIP measurement were the same with those prepared for SEM testing. The maximum pressure for intruding mercury into the pores was 207 MPa. Pore size of 7 nm and up to 150 μm could be measured. The porosity and pore size distribution of the cement mortars were obtained by assuming the pores were cylindrical and the contact angle between mercury and cement paste was 140°.

3. Experimental results and discussion

3.1 Hardened properties

3.1.1 Density and water absorption

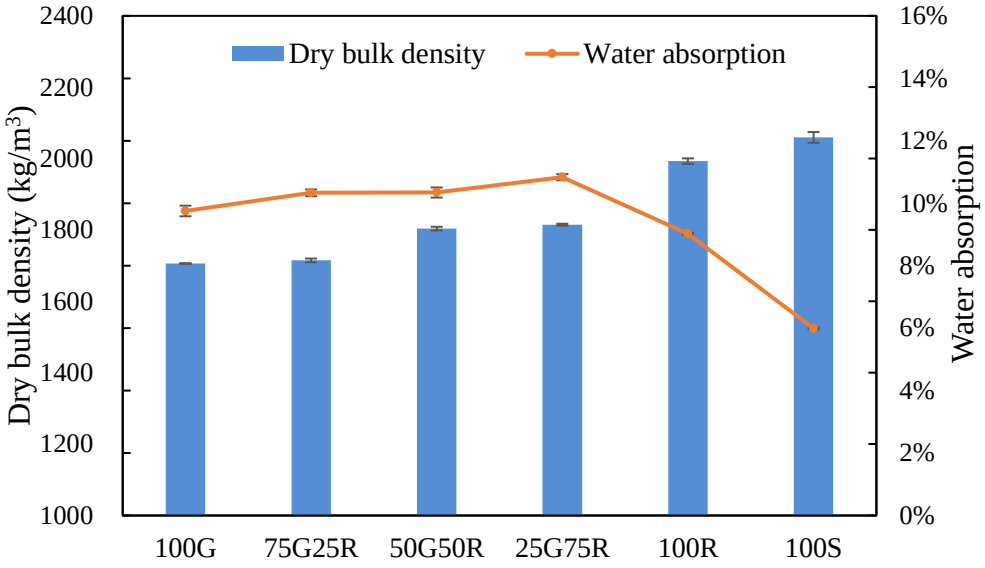

Fig. 6 Effect of RGC and RFA on the density and water absorption of cement mortars

Fig. 6 shows the influence of RGC and RFA contents on the density and water absorption of the cement mortars. The results indicate that the density of the cement mortars increased with increasing replacements of RGC by RFA. The main reason could be the higher intrinsic density of RFA than that of RGC (as shown in Table 2). Another explanation was the higher air content and poorer compaction of the mixture due to the incorporation of RGC as the shape of which was sharper edge and a higher aspect ratio [61, 62]. Especially for the cement mortar prepared with 100% RFA, an obvious increase in the density was observed, which means a higher compaction of the 100R mixture. As compared to the RGC-RFA cement mortar, the 100% RS sample had a higher density which might be attributed to the finer particle size of RS (see Fig. 2b) and the relatively round shaped particle of natural sand [63] enabling better packing [64].

For the water absorption results, it can be observed that the value increased when the RGC was replaced by RFA up to 75%, whereas an apparent drop was noticed as the RFA replacement reached 100% of the aggregates. Generally, the water absorption of

concrete is reduced with the increase of concrete density [65, 66]. In this study, two factors affected the water absorption of the cement mortars. One is the increasing content of RFA would bring about a higher entire water absorption of the cement mortar owing to the replacement of RGC (negligible sorptivity) by RFA (higher sorptivity) (as indicated in Table 2). On the other hand, the water absorption value of the cement mortar was reduced with the increased density by incorporating RFA (density results) as water was more difficult to penetrate into the denser matrix. Given the effect of former factor, the water absorption of the cement mortar gradually increased when the content of RFA was less than 75%. However, when the RGC was fully replaced by the RFA, the latter factor would exert a more dominant role in controlling the water absorption of the cement mortar. As expected, a further reduction in the water absorption can be found in the 100% RS mortar due to the low water absorption of RS and much higher density of the matrix.

3.1.2 Compressive strength

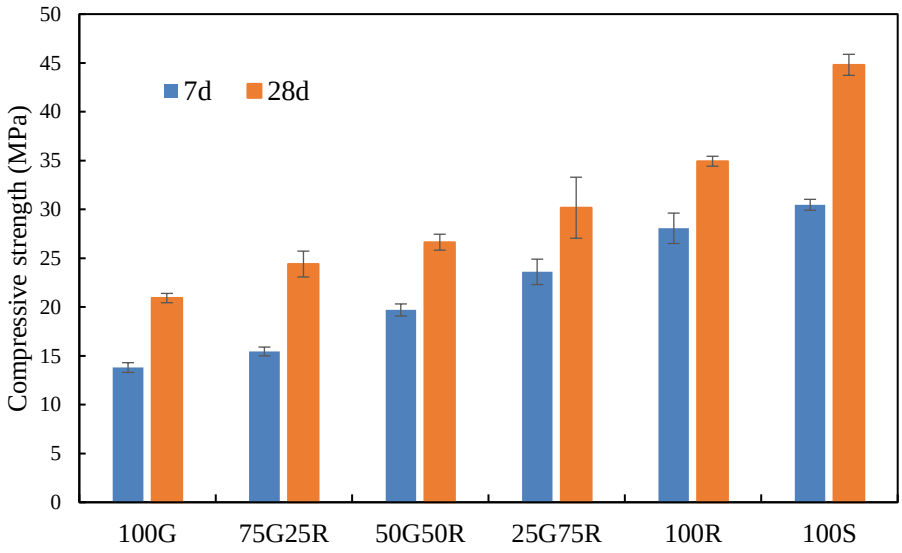

Fig. 7 Effect of RGC and RFA on the compressive strength of cement mortars

Fig. 7 shows the effect of increasing RFA contents on the compressive strength of the cement mortars. Obviously, the compressive strength increased with the increase of RFA replacement content, regardless of the curing ages. The enhancement of strength was consistent with the increased density results. Generally, the incorporation of RGC with smooth surfaces would reduce the strength of the cement mortar/concrete [20, 67]. Also, the contaminants in the RGC (e.g. papers in Fig. 3) might have adverse effects on

the strength development. Therefore, replacing RGC by RFA with rough surfaces was expected to enhance the strength by improving the bonding strength. This will be further discussed in the microstructure analysis section. Furthermore, considering the relatively higher water absorption of RFA (see Table 2), the substitution of RFA for RGC was also beneficial to increasing the strength of the cement mortar due to a lower effective *w*/*b* ratio. For the cement mortars containing 100% RS, the compressive strength was the highest compared to the mortars containing RGC and RFA. Little contamination in RS might be a reason for the high strength. Another explanation could be attributed to the relatively round shape and low fineness modulus of RS in comparison with that of RGC and RFA (as shown in Fig. 2b), which facilitated to achieve good packing.

3.2 Durability properties

3.2.1 Drying shrinkage

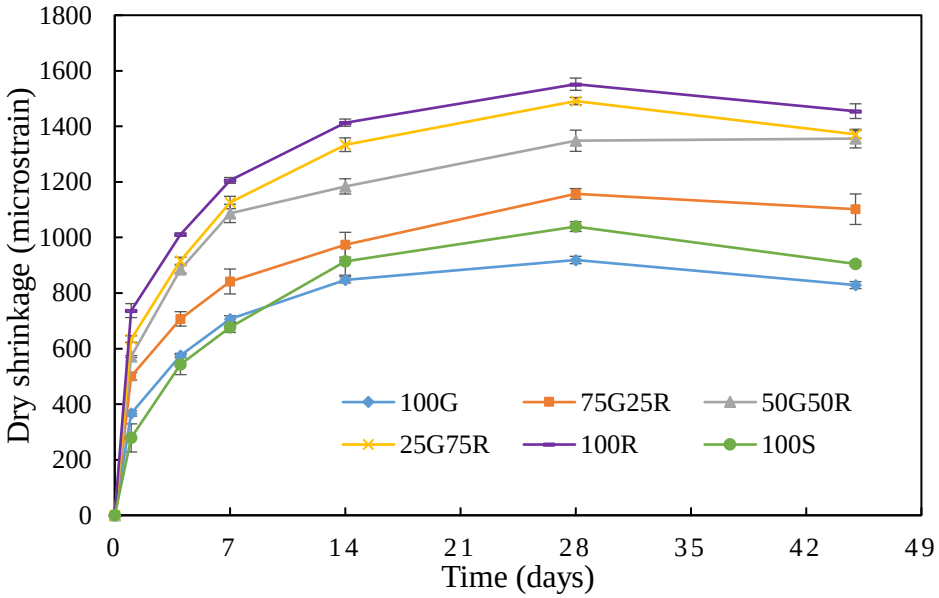

Fig. 8 Effect of RGC and RFA on the drying shrinkage of cement mortars

The influence of the varying RFA contents on the volume change of the cement mortars are shown in Fig. 8. All the cement mortars suffered some shrinkages within the first 14 days and then the shrinkage was stabilized. It should be pointed out that the total drying shrinkage measured in this study also included the autogenous shrinkage arising from the continued hydration (chemical shrinkage) and withdrawal of water from the capillary pores (self-desiccation). Apart from the water evaporation caused by drying

condition, the volume changes due to the early hydration and self-desiccation were also responsible for the shrinkage during the early age. Obviously, with increasing replacement of RGC by RFA, the volume contraction of the cement mortars increased accordingly. This might be associated with the higher water absorption of RFA, which reduced the effective *w*/*b* ratio in the mixture. As indicated by the study of Zhang et al. [68], a decreasing *w*/*b* ratio would increase the autogenous shrinkage. Therefore, the higher autogenous shrinkage due to the replacement of RGC by RFA partly resulted in a higher total shrinkage. Another possible explanation was the use of RFA containing a large proportion of fine particles smaller than 75 μm (see Table 2) could cause a higher shrinkage as the fines would result in a larger void content [69].

On the contrary, it can be easily observed that when more RGC was used in the cement mortar, less drying shrinkage would occur. The non-hydroscopic nature of RGC was beneficial to reducing the drying shrinkage of the cement mortars. Also, the high hardness of glass was conducive to enhancing restraints against drying condition. In consequence, the cement mortar prepared with 100% RGC had a lower drying shrinkage than that prepared with 100% RS. Similar results were also reported by previous works in mortars or concrete prepared with glass aggregates [11, 70].

However, for the combined use of RGC and RFA in the cement mortar, the ultimate drying shrinkage values were still higher than that of the 100% RS mixed cement mortar. The Australian Standard [71] recommended that the volume change of concrete derived from the drying shrinkage should be less than 1000 με. For potential application of RGC and RFA in cement mortars, clean RGC washed by tap water was used in cement mortar in order to further reduce the total drying shrinkage. As presented in Fig. 9, after 45 days of drying, the total shrinkages of the cement mortars prepared with 100% RGC and 50%RGC-50%RFA could be effectively reduced to 673 με and 930 με, respectively. The benefit can be explained by removing most of the contaminants (papers) in the RGC. Overall, the joint utilization of 50% RGC and 50% RFA as fine aggregates could successfully limit the shrinkage of the cement mortars to within an acceptable requirement, and consequently reducing the risk of cracking.

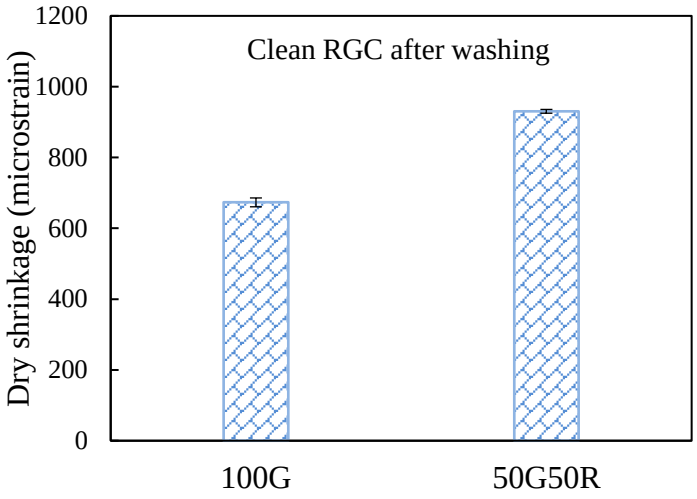

Fig. 9 Drying shrinkage of cement mortars incorporating clean RGC (after washing by tap water) and RFA

3.2.2 Alkali-silica reaction

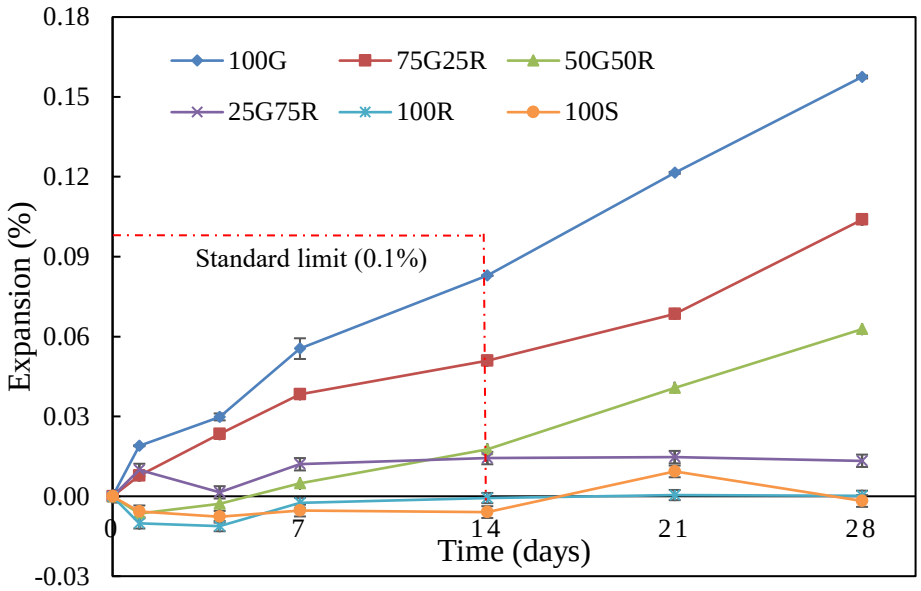

Fig. 10 Effect of RGC and RFA on the ASR expansion of cement mortars

The major concern on recycling RGC as aggregates in cement mortars is the potential deterioration due to the ASR expansion as the glass is rich in amorphous silica (see Table 1 and Fig. 4b). Fig. 10 presents the influence of RGC and RFA additions on the ASR expansion of cement mortars. As envisaged, the expansion of mortars was reduced with the decreasing content of RGC and the increasing content of RFA. When the proportion of RFA was higher than 75% of the total aggregates, the volumetric

dilatation of mortars was negligible and comparable to that of mortar prepared with RS. The benefits of incorporating RFA and RS in the alkaline environment were attributed to their stable crystalline structures as indicated in the XRD results. However, it is worth noting that, although the RGC was utilized as 100% aggregates in the cement mortar, the ASR expansion at 14 days was still below 0.1%, which is the threshold value recommended by the ASTM C1260. The addition of 20% GGBS as a replacement of cement was responsible for the mitigation of ASR dilatancy [19]. Even so, a significant increase in the expansion was noticed at a prolonged test duration when the amount of RGC was in excess of 50%. Thus, given the detrimental effect of ASR due to the RGC incorporation, more SCM should be introduced into the cement mortars to avoid this issue.

3.2.3 High temperature resistance

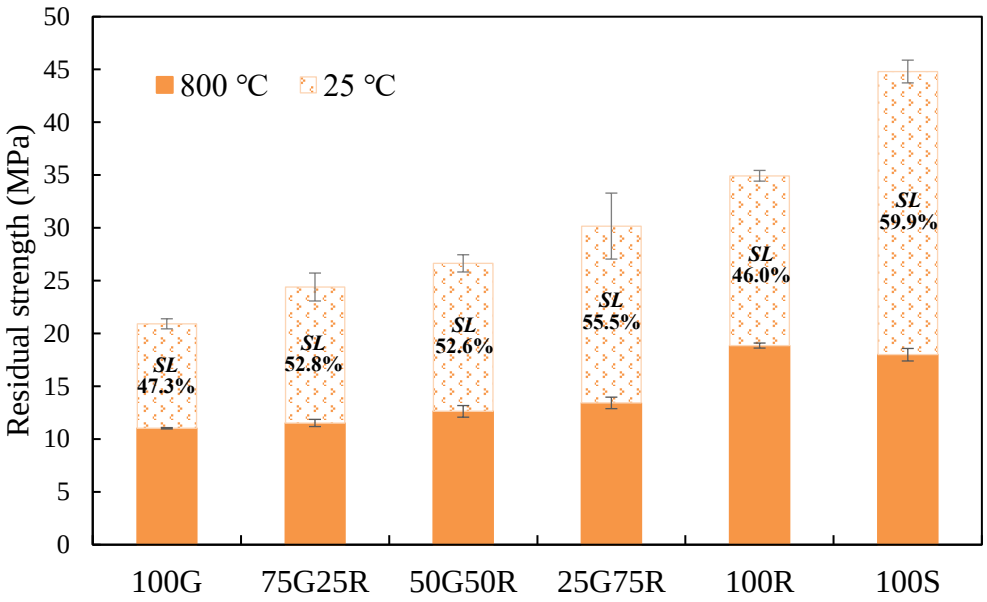

Fig. 11 Effect of RGC and RFA on the high temperature resistance of cement mortars

The high temperature resistance ability of the cement mortars prepared with RGC and RFA is illustrated in Fig. 11. After the elevated temperature exposure, all the cement mortars experienced severe deterioration in strength due to the decomposition of the cement hydration products. As mentioned before, the initial compressive strength (at ambient temperature) of the cement mortar increased with increasing RFA content. After subjected to the elevated temperature (800 °C), the residual strength of the mortars containing a higher amount of RFA was still higher than that incorporated with

a high amount of RGC. However, the percentage strength loss of the mortars incorporating more RGC was lower than that of the mortars prepared with more RFA (except 100% RFA mixed mortar). The less strength loss is thought to be related to the phase transition of the glass cullet at high temperature. As indicated in DTA result (see Fig. 5), the glass transition temperature of the soda-lime silica glass was at below 700 °C. This means that the RGC experienced transition from rigid state to more flexible state when exposed to 800 °C. It can be anticipated that the glass particles would be softened/melted to bond the decomposed binder around the RGC aggregates. After cooling down, this would improve the ITZ between the cement paste and the RGC [72]. The result was consistent with the findings of a previous study [61], indicating that the introduction of RGC improved the fire resistance of concrete after exposure to high temperatures.

It should be noticed that the mortar mixed with 100% RS suffered a considerable drop of strength after exposure to 800 °C which was higher than other mortars prepared with RGC and RFA. This might be due to the thermal expansion mismatch between the cement paste and the quartz in the RS. The thermal expansion coefficient of quartz (18×10^{-6}/°C) was much higher as compared to that of glass ($7–9 \times 10^{-6}$/°C) [73]. More importantly, the volume change of quartz at 573 °C from β-form to α-form after cooling down caused damages of ITZ [74], and consequently led to strength deterioration. However, for the mortar prepared with 100% RFA, the degradation in the strength was relatively lower, which means a better resistance to high temperature. This could be explained by the lower amount of quartz phase in the RFA as shown in composition and mineralogy results, thus leading to low impacts from phase conversion (see DTA result) in comparison with the RS. Another explanation was interpreted to the different thermal expansion coefficients of quartz in the RS and granite in the RFA. According to the study of Tufail et al. [75], the quartz-based concrete exhibited a higher volume expansion than granite concrete because granite (less quartz) had a lower coefficient of thermal expansion than quartzite. Nonetheless, the quartz content in the RFA was still much higher than the RGC without quartz. This was also one reason why the increasing content of RFA in the mortar caused higher percentage of strength loss. However, it was found that the 100R experienced the lowest strength loss among all the mixtures despite the RFA contained a certain amount of quartz. It should be noted that, apart from quartz, muscovite was also an important component in the RFA. The well-crystallized muscovite was reported to have a strong resistance to thermal decomposition at high

temperatures [54]. Therefore, the presence of muscovite might mitigate the strength deterioration resulting from the quartz inside. Furthermore, the higher porosity and a large number of fine pores in the 100R was also likely to relieve partial expansion stress and reduced the strength loss.

3.2.4 Acid resistance

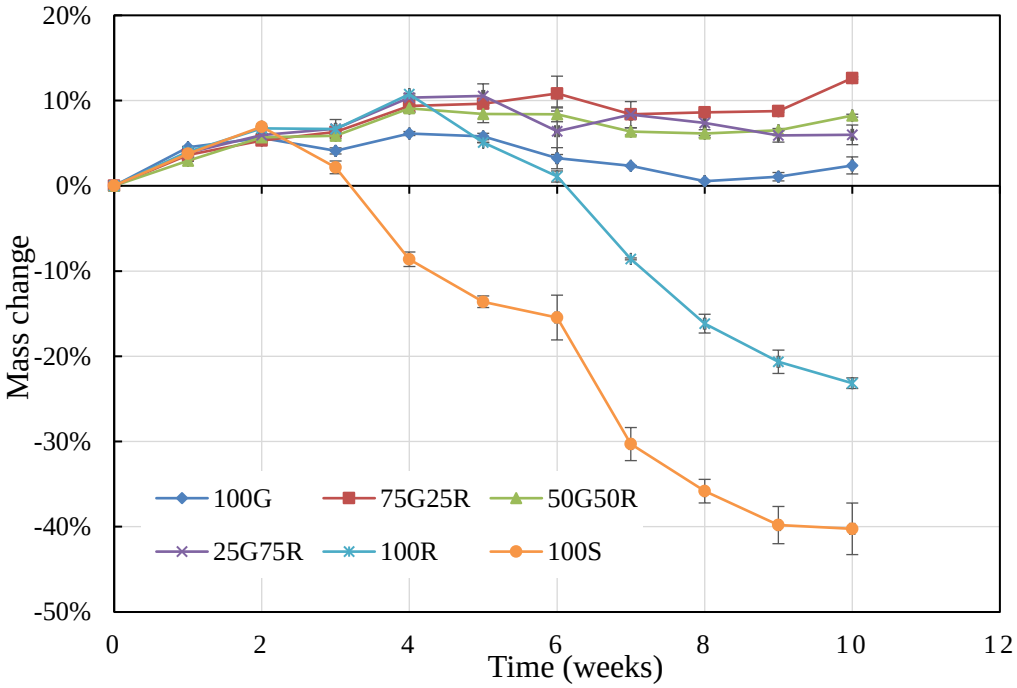

Fig. 12 Effect of RGC and RFA on the acid resistance of cement mortars

Mass variation is an indicator for assessing the resistance of cement mortars to acid attack. Thus, the cumulative mass loss of the specimens after immersing in the sulfuric acid solution represents the successive decomposition of the cement mortars. The mass change profile of the cement mortars containing RGC and RFA during the acid attack is plotted in Fig. 12. Initially, the weights of all the mortars increased. The generation of secondary ettringite ($C_3A{\cdot}3CaSO_4{\cdot}32H_2O$) and gypsum ($CaSO_4{\cdot}2H_2O$) [76] due to the reaction between the hydration products and sulfate ions on the mortar surfaces was the primary reason. After 4 weeks of exposure to the acidic medium, the mortar incorporating 100% RS incurred a dramatic loss in mass, while other mortars prepared with RGC and RFA still experienced mass gains. The remarkable decrease in mass of 100S was related to expansive deterioration due to the formation of excessive gypsum and ettringite [77]. As known, sulfuric acid would exert very aggressive attack on the alkaline cement-based materials because of a dual chemical aggressiveness of acid

attack and sulfate attack [78]. The decomposition of larger number of hydration products on the mortar surface would cause losing of adhesion between the aggregates.

Similarly, the cement mortar containing 100% RFA also suffered considerable degradation in mass after exposure to the sulfuric acid solution for 7 weeks. However, the deterioration of the 100R mortar was significantly delayed in comparison with the 100S mortar. Similar results were also reported by [79], which found that the use of fine granite aggregates as a replacement of RS in the concrete could improve the resistance against sulfate attack. The delayed mass loss of 100R was probably attributed to a certain content of the fine granite particles in the RFA (see Table 2) could increase the resistance to acid attack [80, 81].

Unexpectedly, Fig. 12 also shows no mass loss was suffered by the cement mortars produced with RGC after 10 weeks of acid exposure. This implies that the glass-mixed mortars exhibited very good resistance to the acid attack. The main reason was that the presence of glass aggregates or the pozzolanic reaction of fine glass particles in the cement mortars were beneficial to resist the sulfuric acid attack. The result was in agreement with the findings of Ling et al. [12], who indicated that the mass loss caused by acid attack decreased with increasing contents of RGC in the cement mortars, but a significant mass deterioration was still found when the RGC was used as a substitute of 100% RS. In this study, a slight increase in mass was observed for the 100G sample after the acid exposure. Comparing with the results of [12], the improved acid resistance of 100G in this work might be partly due to the original inclusion of GGBS in the cement mortar, which had been proven to be effective in resistance against the sulfuric acid solution because less calcium hydroxide was formed in the cementitious matrix [82]. However, the addition of GGBS was still not the dominant factor in controlling the mass loss in acidic environment as the RGC and RFA mixed mortars also incorporated with the same GGBS content. It is worth noting that the RGC contained a certain amount of glass powder (as seen in Table 2), which had been demonstrated to have a good resistance against acid attack [83, 84]. The superior acid resistance of 100G could be explained from three aspects: 1) the fine glass powder with pozzolanic reactivity in the RGC could consume some calcium hydroxide, which is usually the most vulnerable cement hydration product with respect to acid attack [83, 84]; 2) the formation of a low Ca/Si C-S-H gel due to the pozzolanic reaction of glass particles could improve the acid resistance [77, 85]; 3) according to the investigation of Siad and

590 his colleagues [84], the reduced formation of ettringite due to the low amount of
591 aluminum in the glass material and binding of the alkalis in the matrix due to the
592 hydration products of glass powder could further mitigate the deterioration of acid
593 attack.
594
595 Contrary to expectation, the combined use of RGC and RFA in the cement mortars was
596 able to provide very good resistance to acid attack and no significant change in the mass
597 was noticed. The concurrent presence of fine glass and granite particles might be
598 conducive to creating barriers to resist the diffusion of acid into the mortar surface,
599 slowing down the degradation rate. The formation of an expanded outer shell on the
600 surface of the mortars (deteriorated zone) was also expected to act as a protective layer
601 to impede the detachment of aggregates and mitigate the propagation of acid. Apart
602 from the positive effects of fine glass particles in the RGC, the coarser size and more
603 irregular shape of RGC and RFA in comparison with the RS (see Table 2) could also
604 slow down the rate of attack as the aggressive ions had to penetrate through longer paths
605 around aggregates to react with cementitious matrix. This explanation was supported
606 by a previous study [77], which indicated that the increasing content of coarse
607 aggregates was effective in improving the resistance to sulfuric acid because of the
608 mitigated reaction between cementitious material and acid ion. Therefore,, the joint
609 utilization of RGC and RFA could contribute to a much better chemical resistance of
610 the cement mortars.
611

3.3 Microstructure analysis

3.3.1 Morphology of ITZ

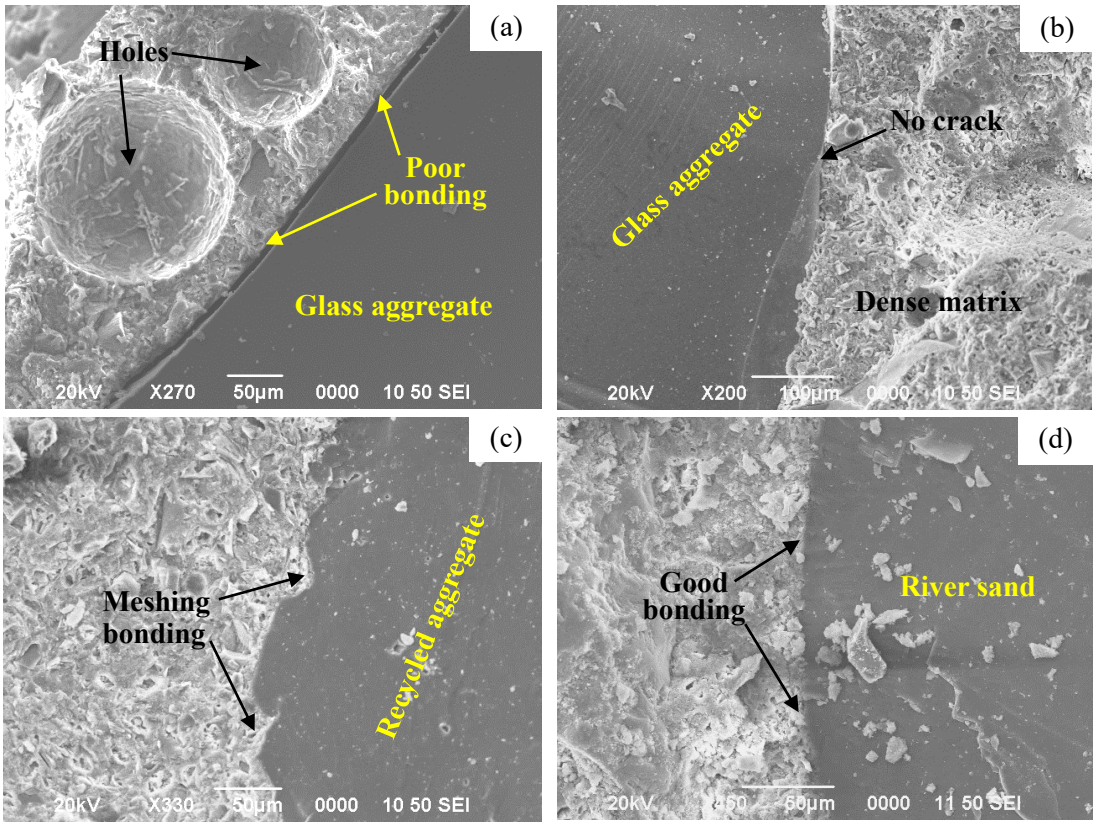

Fig. 13 SEM of cement mortars prepared with RGC, RFA and RS, (a) 100G (b) 50G50R (c) 100R (d) 100S

Due to the higher porosity of the matrix formed near the aggregates, the ITZ is usually known to be the weakest zone of the concrete associated with negative impacts on durability [86]. Thus, understanding the interfacial morphology is helpful to explain the mechanical and durability properties of the produced cement mortars. Intuitively, for the mortar prepared with 100% RGC (Fig. 13a), the interfacial zone between the glass aggregate and the cement paste was weak due to the presence of visual cracks. Moreover, there were large voids present near the glass particle. This phenomenon verified the high porosity of the ITZ and implied more porous areas surrounding the glass aggregates. The poor bonding between the aggregates and the cement matrix was the reason why the GC mortars had lower compressive strength than other mortars. Furthermore, the porous interfacial zone was believed to be permeated preferentially and subsequently effect the transport properties of cement mortar [87]. As the glass had non-absorbent nature and smooth surface, it was prone to form a water-rich zone around the RGC particles due to the wall effect [88]. This might render the bleeding around

glass aggregates.

After introducing 50% RFA into the cement mortar (Fig. 13b), it can be observed that no crack was present in the interface of the glass-paste, and the cement paste matrix surrounding the aggregate surface was dense with few voids. This implies that the ITZ was improved by partial replacement of RGC by RFA. The beneficial behavior could be explained by that the addition of RFA reduced the available free water in the vicinity of the glass aggregates due to the higher water absorption of RFA (see Table 2). As a result, the combined use of RGC and RFA was conducive to mitigating the poor bonding between the glass particles and cement paste, thus resulting in a better strength of the cement mortar. Fig. 13c shows the ITZ of the cement mortar prepared with 100% RFA as the aggregate, which clearly demonstrated an interlocking interface between the aggregate-paste. Since the RFA had rough surface with convexity and concavity, the hydration products, mostly like C-S-H gel, could fill into the concave corners to make the connection of cementitious matrix with RFA well-bonded. Also, it should be noted that the paste matrix nearby the RFA particle was more compact in comparison with that containing RGC. This phenomenon was thoughted to be the following reasons: 1) a certain content of fine particles in the RFA, such as crusher dust, required more water in the mix to wet the particles surfaces, thereby reducing the effective *w*/*b* ratio of the cementitious matrix; 2) the inclusion of fine particles less than 75 μm could act as a filler to reduce the voids content in the mixture [89]; 3) the small-scale protrusions and indentations on the surface of RFA increased the specific surface area of aggregates, thus alleviating the water bleeding on the boundary of the aggregates. Such above effects were accompanied by reducing porosity in the ITZ and improving the interlocking ability of the aggregates, consequently, resulting in a densification of microstructure and enhancement of compressive strength.

Also, it can be seen from Fig. 13d that the paste-sand interfacial zone was well-defined, whereas no crack and void was found in the zone. Compared to the meshing bonding of the RFA mixed mortar due to RFA's rough surface, the rounded shape and smooth texture of RS led to a smoother contact surface with the cement paste. Bonding failure was more likely to take place along the central 'equatorial' zone for sphere aggregates under compression-shear load [90]. Nonetheless, since RS possessed smaller particle size than the RFA and the RGC, the thickness of ITZ would be less than the larger aggregate particles [91]. This might be one reason why the compressive strength of the

cement mortar prepared by using RS still had the highest value.

3.3.2 Microhardness

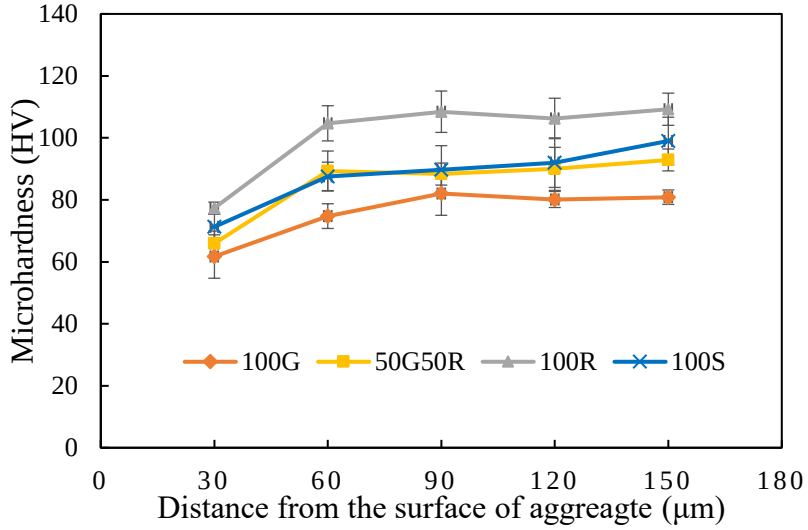

Fig. 14 Vickers microhardness at ITZ of cement mortars prepared with RGC, RFA and RS

The microhardness values across the ITZ between the aggregates and the cement pastes in the cement mortars are shown in Fig. 14. Moreover, the microhardness values of the separately tested RGC, RFA, RS in the cement mortars were 739±43, 785±56, 770±28, respectively. Generally, a denser material would increase the microhardness value. Hence, the microhardness of the aggregates was much higher than that of the ITZ and the cement paste. Also, it is clearly shown that the microhardness values of the cement pastes in the immediate vicinity of the aggregate surfaces were lower than those located further away. In particular, the ITZ of 100G was the weakest, which was consistent with the porous interfacial zone of the sample revealed by SEM observation. Nonetheless, with the increasing addition of the RFA, the microhardness of the area in the vicinity of aggregate was increased. This indicates that the presence of the RFA was conducive to improving the ITZ. Furthermore, it can be seen that with an increasing amount of RFA, the hardness values of the bulk paste became higher, which confirmed the denser microstructure observed by the SEM results when compared to the case of the 100G. As mentioned above, the reduced effective *w*/*b* ratio and filling effect by the fine particles of RFA might be the reasons. For the 100S mortar, the microhardness value on the paste matrix was comparable to the 50G50R although the use of RS could facilitate a better ITZ. This result implies that the strength of 100S was not mainly dependent on

the strength of the cement paste. The better packing and the reduction of ITZ thickness might also contribute to the strength development of the RS mortar.

3.3.3 Pore structure

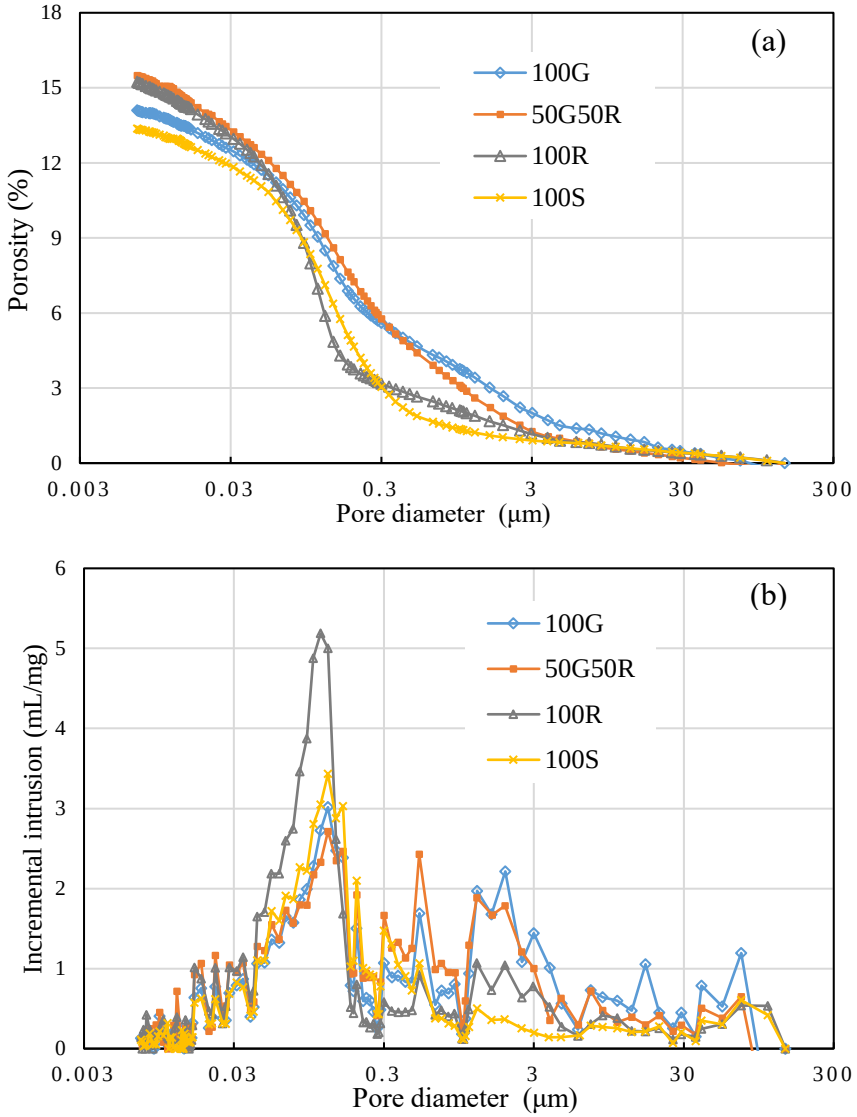

Fig. 15 Pore structure of cement mortars prepared with RGC, RFA and RS, (a) porosity (b) pore size distribution

In order to better understand the influence of the WGC and RFA replacement on the pore structure of the cement mortars, MIP test was employed to analyze the porosity and pore size distribution. Fig. 15a shows the porosity of the cement mortars. In general, a lower porosity leads to better mechanical properties [92]. It can be clearly seen that the mortar prepared with 100% RS had the lowest porosity (13.4%), which

corresponded to its highest strength (Fig. 7). However, although the strength of 100R sample was higher than that of 100G sample, the porosity of former (15.2%) was higher than that of latter (14.1%). The reason was attributed to the presence of a larger number of fine pores in 100R. Fig. 15b shows the pore size distribution of the cement mortars. There were many large pores present in the 100G sample. With 50% RFA addition, the percentage of these larger pores (>3 μm) was reduced. By fully replacing RGC by RFA, this part of the large pores was further reduced. Particularly, when compared to 100G, the critical pore diameter shifted towards the left side for 100R, implying that the large pores were changed into fine pores. As a result, the average pore diameter was reduced from 74.3 nm to 56.0 nm. This refinement of the pore structure partly explained that increasing the content of RFA increased the strength of the cement mortar. As indicated by ITZ images (Fig. 13), the elimination of pores and cracks in the vicinity of RGC could be one reason for the reduced pore size. Another explanation might be due to the lower effective *w*/*b* ratio of the bulk paste resulting from the higher water absorption of RFA, which refined the pores. These results were consistent with the higher density and lower water absorption of the 100R mortar mentioned before. The incorporation of RFA containing some fine particles (<75 μm) to the cement mortar also improved the impermeability of the matrix because the fine particles could block the passages connecting the capillary pores and water channels. The increased content of the capillary pores in the 100R mortar also induced a higher shrinkage (see Section 3.2.1) [61].

For the pore size distribution of the cement mortar prepared with 100% RS as the aggregate, a significant reduction in the number of large pores was resulted as shown in Fig. 15b. This result was in accordance with the lower porosity of the 100% RS mortar. The reduced content of detrimental coarse pores was partly responsible for the reduction of water absorption and the enhancement of compressive strength. The reason was considered to be the good packing of the constitutes of mixture due to the round and fine geometry of the sand grains. It should be noted that the use of 100% RS in the cement mortar indeed reduced the fraction of large pores (>1 μm), while it did not significantly increase the quantity of small pores (<300 nm) as compared to the 100G. Hence, this refinement of the pore structure in the 100S sample did not contribute to higher drying shrinkage.

5. Conclusions

The shortage of natural sand for producing cement mortar/concrete attracts great interests in exploring the feasibility of using recycled aggregates in the manufacture of cement-based construction products. This study provides insight into the potential of recycling of RGC and RFA concurrently for preparing cement mortars. The synergetic effects of replacement of RGC with RFA on the hardened, durability and microstructural properties of cement mortars were evaluated. From the experimental investigation, the following conclusions can be drawn:

- Making use of the characteristics of two recycled aggregates, the proper co-reuse of RGC and RFA could counteract the adverse effects of each other to maintain the appropriate fresh properties (workability) of the cement mortars. For hardened properties, the dry bulk density of the cement mortars increased with increasing replacements of RGC by RFA due to the higher intrinsic density of RFA than that of RGC and the higher compaction of RFA containing mixture. Moreover, the increasing substitution of RFA for RGC in the cement mortar led to increase of the compressive strength. Hence, the combined recycling of RGC and RFA together could mitigate the inferior strength induced by RGC.

- The combined utilization of RGC and RFA as fine aggregates can offset the high drying shrinkage of the cement mortars caused by the inclusion of RFA alone. With increasing replacement of RGC by RFA, the ASR expansion of cement mortars decreased significantly to below the threshold value recommended by construction standards.

- After exposure to high temperature, the cement mortar prepared with 100% RS suffered significant loss in strength due to the volume changes of quartz at 573 °C. However, the incorporation of RGC and RFA was able to improve the fire resistance of the mortar because of the phase reversibility of the glass materials at high temperature and the lesser amount of quartz in RFA. Especially, the cement mortars prepared with RGC exhibited excellent resistance to acid attack due to the pozzolanic reaction of fine glass particles in the RGC and relatively coarser size of RGC.

- The inclusion of 100% RGC in the cement mortar induced a higher porosity around ITZ and resulted in poorer bonding between the paste and the aggregates. In contrast, the incorporation of RFA contributed to an interlocking interface in the aggregate-paste zone. Thus, the combined use of RGC and RFA was beneficial to improving the bonding of ITZ and increasing the microhardness of the area in the vicinity of aggregate. When compared with 100% RGC mortar, the joint introduction of RFA and RGC could reduce the quantity of larger pores and resulted in higher strength.

Acknowledgements

The authors wish to thank the financial supports of the Environment and Conservation Fund, the Environmental Protection Department, and the Civil Engineering and Development Department of the Hong Kong SAR Government. Special thanks are due to Ms. Dorothy Ho-Yee Chan (The Hong Kong Polytechnic University) for her warm assistance with XRF and TG measurements. Also, we are grateful to all the anonymous reviewers for their valuable comments and precious time for improvement of the manuscript.

References

[1] A. Jesse, Sand mining at Poyang Lake, Using Landsat data from the U.S. Geological Survey, NASA Earth Observatory (2016).
[2] X. Lai, D. Shankman, C. Huber, H. Yesou, Q. Huang, J. Jiang, Sand mining and increasing Poyang Lake's discharge ability: A reassessment of causes for lake decline in China, Journal of Hydrology, 519 (2014) 1698-1706.
[3] J. Yao, D. Zhang, Y. Li, Q. Zhang, J. Gao, Quantifying the hydrodynamic impacts of cumulative sand mining on a large river-connected floodplain lake: Poyang Lake, Journal of Hydrology, 579 (2019).
[4] J. de Leeuw, D. Shankman, G. Wu, W.F. de Boer, J. Burnham, Q. He, H. Yesou, J. Xiao, Strategic assessment of the magnitude and impacts of sand mining in Poyang Lake, China, Regional Environmental Change, 10 (2009) 95-102.
[5] Y. Chen, C. Guo, S. Ye, F. Cheng, H. Zhang, L. Wang, R.M. Hughes, Construction limit China's sand mining, Nature, 550 (2017) 457.
[6] B. Mette, B. Jim, H. Chris, I. Lars Lønsmann, Time is running out for sand, Nature comment, (2019).
[7] Environmental Protection Department, Monitoring of Solid Waste in Hong Kong, Waste Statistics, (1997-2017).

[8] J.-X. Lu, C.S. Poon, Recycling of waste glass in construction materials, in: New Trends in Eco-efficient and Recycled Concrete, 2019, pp. 153-167.
[9] S. Chandra Paul, B. Šavija, A.J. Babafemi, A comprehensive review on mechanical and durability properties of cement-based materials containing waste recycled glass, Journal of Cleaner Production, 198 (2018) 891-906.
[10] M.N.N. Khan, A.K. Saha, P.K. Sarker, Reuse of waste glass as a supplementary binder and aggregate for sustainable cement-based construction materials: A review, Journal of Building Engineering, 28 (2020) 101052.
[11] J.-X. Lu, H. Zheng, S. Yang, P. He, C.S. Poon, Co-utilization of waste glass cullet and glass powder in precast concrete products, Construction and Building Materials, 223 (2019) 210-220.
[12] T.-C. Ling, C.-S. Poon, S.-C. Kou, Feasibility of using recycled glass in architectural cement mortars, Cement and Concrete Composites, 33 (2011) 848-854.
[13] M.J. Terro, Properties of concrete made with recycled crushed glass at elevated temperatures, Building and Environment, 41 (2006) 633-639.
[14] H.Y. Wang, A study of the effects of LCD glass sand on the properties of concrete, Waste Management 29 (2009) 335-341.
[15] S.C. Kou, C.S. Poon, Properties of self-compacting concrete prepared with recycled glass aggregate, Cement and Concrete Composites, 31 (2009) 107-113.
[16] H. Siad, M. Lachemi, M. Sahmaran, H.A. Mesbah, K.M. Anwar Hossain, A. Ozsunar, Potential for using recycled glass sand in engineered cementitious composites, Magazine of Concrete Research, 69 (2017) 905-918.
[17] H. Siad, M. Lachemi, M. Sahmaran, H.A. Mesbah, K.M.A. Hossain, Use of recycled glass powder to improve the performance properties of high volume fly ash-engineered cementitious composites, Construction and Building Materials, 163 (2018) 53-62.
[18] H. Siad, M. Lachemi, M. Sahmaran, K.M.A. Hossain, Mechanical, Physical, and Self-Healing Behaviors of Engineered Cementitious Composites with Glass Powder, Journal of Materials in Civil Engineering, 29 (2017) 04017016.
[19] J.-X. Lu, B.-J. Zhan, Z.-H. Duan, C.S. Poon, Improving the performance of architectural mortar containing 100% recycled glass aggregates by using SCMs, Construction and Building Materials, 153 (2017) 975-985.
[20] K.H. Tan, H. Du, Use of waste glass as sand in mortar: Part I – Fresh, mechanical and durability properties, Cement and Concrete Composites, 35 (2013) 109-117.
[21] B. Taha, G. Nounu, Using lithium nitrate and pozzolanic glass powder in concrete as ASR suppressors, Cement and Concrete Composites, 30 (2008) 497-505.
[22] B.J. Zhan, D.X. Xuan, W. Zeng, C.S. Poon, Carbonation treatment of recycled concrete aggregate: Effect on transport properties and steel corrosion of recycled aggregate concrete, Cement and Concrete Composites, 104 (2019) 103360.
[23] H. Zhang, T. Ji, H. Liu, S. Su, Modifying recycled aggregate concrete by aggregate surface treatment using sulphoaluminate cement and basalt powder, Construction and Building Materials, 192 (2018) 526-537.

838 [24] C. Thomas, J. de Brito, A. Cimentada, J.A. Sainz-Aja, Macro- and micro-
839 properties of multi-recycled aggregate concrete, Journal of Cleaner Production, 245
840 (2020) 118843.
841 [25] J. Xie, J. Wang, R. Rao, C. Wang, C. Fang, Effects of combined usage of GGBS
842 and fly ash on workability and mechanical properties of alkali activated geopolymer
843 concrete with recycled aggregate, Composites Part B: Engineering, 164 (2019) 179-
844 190.
845 [26] T. Liu, Z. Wang, D. Zou, A. Zhou, J. Du, Strength enhancement of recycled
846 aggregate pervious concrete using a cement paste redistribution method, Cement and
847 Concrete Research, 122 (2019) 72-82.
848 [27] D.X. Xuan, A.A.A. Molenaar, L.J.M. Houben, Shrinkage cracking of cement
849 treated demolition waste as a road base, Materials and Structures, 49 (2015) 631-640.
850 [28] D.X. Xuan, A.A.A. Molenaar, L.J.M. Houben, Compressive and indirect tensile
851 strengths of cement-treated mix granulates with recycled masonry and concrete
852 aggregates, Journal of Materials in Civil Engineering, 24 (2012) 577-585.
853 [29] S. Dadsetan, H. Siad, M. Lachemi, M. Sahmaran, Construction and demolition
854 waste in geopolymer concrete technology: a review, Magazine of Concrete Research,
855 71 (2019) 1232-1252.
856 [30] J. Xiao, W. Li, Y. Fan, X. Huang, An overview of study on recycled aggregate
857 concrete in China (1996–2011), Construction and Building Materials, 31 (2012) 364-
858 383.
859 [31] J.-X. Lu, X. Yan, P. He, C.S. Poon, Sustainable design of pervious concrete using
860 waste glass and recycled concrete aggregate, Journal of Cleaner Production, 234 (2019)
861 1102-1112.
862 [32] C.J. Zega, A.A. Di Maio, Use of recycled fine aggregate in concretes with durable
863 requirements, Waste Management, 31 (2011) 2336-2340.
864 [33] S.T. Lee, Influence of recycled fine aggregates on the resistance of mortars to
865 magnesium sulfate attack, Waste Management, 29 (2009) 2385-2391.
866 [34] L. Evangelista, M. Guedes, J. de Brito, A.C. Ferro, M.F. Pereira, Physical,
867 chemical and mineralogical properties of fine recycled aggregates made from concrete
868 waste, Construction and Building Materials, 86 (2015) 178-188.
869 [35] D. Carro-López, B. González-Fonteboa, J. de Brito, F. Martínez-Abella, I.
870 González-Taboada, P. Silva, Study of the rheology of self-compacting concrete with
871 fine recycled concrete aggregates, Construction and Building Materials, 96 (2015) 491-
872 501.
873 [36] X. Wang, R. Yu, Z. Shui, Q. Song, Z. Liu, M. bao, Z. Liu, S. Wu, Optimized
874 treatment of recycled construction and demolition waste in developing sustainable
875 ultra-high performance concrete, Journal of Cleaner Production, 221 (2019) 805-816.
876 [37] M. Behera, A.K. Minocha, S.K. Bhattacharyya, Flow behavior, microstructure,
877 strength and shrinkage properties of self-compacting concrete incorporating recycled
878 fine aggregate, Construction and Building Materials, 228 (2019).
879 [38] L. Li, B.J. Zhan, J. Lu, C.S. Poon, Systematic evaluation of the effect of replacing

880 river sand by different particle size ranges of fine recycled concrete aggregates (FRCA)
881 in cement mortars, Construction and Building Materials, 209 (2019) 147-155.
882 [39] P. Gonçalves, J.d. Brito, Recycled aggregate concrete (RAC) – comparative
883 analysis of existing specifications, Magazine of Concrete Research, 62 (2010) 339-346.
884 [40] J. Zhang, C. Shi, Y. Li, X. Pan, C.-S. Poon, Z. Xie, Performance enhancement of
885 recycled concrete aggregates through carbonation, Journal of Materials in Civil
886 Engineering, 27 (2015).
887 [41] G. Pan, M. Zhan, M. Fu, Y. Wang, X. Lu, Effect of CO2 curing on demolition
888 recycled fine aggregates enhanced by calcium hydroxide pre-soaking, Construction and
889 Building Materials, 154 (2017) 810-818.
890 [42] G.M. Cuenca-Moyano, M. Martín-Morales, I. Valverde-Palacios, I. Valverde-
891 Espinosa, M. Zamorano, Influence of pre-soaked recycled fine aggregate on the
892 properties of masonry mortar, Construction and Building Materials, 70 (2014) 71-79.
893 [43] Z. Feng, Y. Zhao, W. Zeng, Z. Lu, S.P. Shah, Using microbial carbonate
894 precipitation to improve the properties of recycled fine aggregate and mortar,
895 Construction and Building Materials, 230 (2020).
896 [44] Z. Zhao, S. Wang, L. Lu, C. Gong, Evaluation of pre-coated recycled aggregate
897 for concrete and mortar, Construction and Building Materials, 43 (2013) 191-196.
898 [45] H. Ogawa, T. Nawa, Improving the quality of recycled fine aggregate by selective
899 removal of brittle defects, Journal of Advanced Concrete Technology, 10 (2012) 395-
900 410.
901 [46] H.-S. Kim, J.-M. Kim, B. Kim, Quality improvement of recycled fine aggregate
902 using steel ball with the help of acid treatment, Journal of Material Cycles and Waste
903 Management, 20 (2017) 754-765.
904 [47] G. Santha Kumar, P.K. Saini, S.R. Karade, A.K. Minocha, Chemico-thermal
905 treatment for quality enhancement of recycled concrete fine aggregates, Journal of
906 Material Cycles and Waste Management, 21 (2019) 1197-1210.
907 [48] R.-U.-D. Nassar, P. Soroushian, Strength and durability of recycled aggregate
908 concrete containing milled glass as partial replacement for cement, Construction and
909 Building Materials, 29 (2012) 368-377.
910 [49] V. Letelier, B.I. Henriquez-Jara, M. Manosalva, G. Moriconi, Combined use of
911 waste concrete and glass as a replacement for mortar raw materials, Waste Management,
912 94 (2019) 107-119.
913 [50] N. Arabi, H. Meftah, H. Amara, O. Kebaïli, L. Berredjem, Valorization of recycled
914 materials in development of self-compacting concrete: Mixing recycled concrete
915 aggregates – Windshield waste glass aggregates, Construction and Building Materials,
916 209 (2019) 364-376.
917 [51] N.S. Borodina, G.B. Fershtater, Composition and nature of muscovite in granites,
918 International Geology Review, 30 (1988) 375-381.
919 [52] H.A. Ali, D. Xuan, C.S. Poon, Assessment of long-term reactivity of initially
920 lowly-reactive solid wastes as supplementary cementitious materials (SCMs),
921 Construction and Building Materials, 232 (2020) 117192.

[53] C.A. Sorrell;, H.U. Anderson, Thermal expansion and the high-low transformation in quartz. II. Dilatometrie studies, Journal of Applied Crystallography, 7 (1974) 468.
[54] G. L. Gaines, W. Vedder, Dehydroxylation of muscovite, Nature, 201 (1964) 495.
[55] M. Mirzahosseini;, K.A. Riding, Effect of Combined Glass Particles on Hydration in Cementitious Systems, J. Mater. Civ. Eng. , 27 (2015) 04014190.
[56] M. Mirzahosseini, K.A. Riding, Effect of curing temperature and glass type on the pozzolanic reactivity of glass powder, Cement and Concrete Research, 58 (2014) 103-111.
[57] S. Liu, G. Xie, S. Wang, Effect of curing temperature on hydration properties of waste glass powder in cement-based materials, Journal of Thermal Analysis and Calorimetry, 119 (2014) 47-55.
[58] S. Liu, G. Xie, S. Wang, Effect of glass powder on microstructure of cement pastes, Advances in Cement Research, 27 (2015) 259-267.
[59] F. Rajabipour;, H. Maraghechi;, G. Fischer, Investigating the Alkali-Silica Reaction of Recycled Glass Aggregates in Concrete Materials, J. Mater. Civ. Eng. , 22 (2010) 1201-1208.
[60] R. Chaïd, S. Kenaï, H. Zeroub, R. Jauberthie, Microstructure and permeability of concrete with glass powder addition conserved in the sulphatic environment, European Journal of Environmental and Civil Engineering, 19 (2014) 219-237.
[61] J.-X. Lu, C.S. Poon, Recycling of waste glass in construction materials, In: New Trends in Eco-efficient and Recycled Concrete, (2019) 153-167.
[62] S.B. Park, B.C. Lee, J.H. Kim, Studies on mechanical properties of concrete containing waste glass aggregate, Cement and Concrete Research, 34 (2004) 2181-2189.
[63] H. He, L. Courard, E. Pirard, F. Michel, Shape analysis of fine aggregates used for concrete, Image Anal Stereol, 35 (2016) 159-166.
[64] A.K.H. Kwan, C.F. Mora, Effects of various, shape parameters on packing of aggregate particles, Magazine of Concrete Research, 53 (2001) 91-100.
[65] M.L. Torres, P.A. García-Ruiz, Lightweight pozzolanic materials used in mortars: Evaluation of their influence on density, mechanical strength and water absorption, Cement and Concrete Composites, 31 (2009) 114-119.
[66] E.K.K. Nambiar, K. Ramamurthy, Influence of filler type on the properties of foam concrete, Cement and Concrete Composites, 28 (2006) 475-480.
[67] İ.B. Topçu, M. Canbaz, Properties of concrete containing waste glass, Cement and Concrete Research, 34 (2004) 267-274.
[68] M.H. Zhang, C.T. Tam, M.P. Leow, Effect of water-to-cementitious materials ratio and silica fume on the autogenous shrinkage of concrete, Cement and Concrete Research, 33 (2003) 1687-1694.
[69] A.M. Neville, Properties of Concrete, John Wiley and Sons Inc., (1996) New York.
[70] H.-Y. Wang, W.-L. Huang, Durability of self-consolidating concrete using waste LCD glass, Construction and Building Materials, 24 (2010) 1008-1013.
[71] P.J.M. Monteiro, G. Geng, D. Marchon, J. Li, P. Alapati, K.E. Kurtis, M.J.A. Qomi, Advances in characterizing and understanding the microstructure of cementitious

964 materials, Cement and Concrete Research, 124 (2019) 105806.
965 [72] S. Yang, T.-C. Ling, H. Cui, C.S. Poon, Influence of particle size of glass
966 aggregates on the high temperature properties of dry-mix concrete blocks, Construction
967 and Building Materials, 209 (2019) 522-531.
968 [73] J.-X. Lu, C.S. Poon, Use of waste glass in alkali activated cement mortar,
969 Construction and Building Materials, 160 (2018) 399-407.
970 [74] L. Zuda, Z. Pavlík, P. Rovnaníková, P. Bayer, R. Černý, Properties of alkali
971 activated aluminosilicate material after thermal load, International Journal of
972 Thermophysics, 27 (2006) 1250-1263.
973 [75] M. Tufail, K. Shahzada, B. Gencturk, J. Wei, Effect of elevated temperature on
974 mechanical properties of limestone, quartzite and granite concrete, International
975 Journal of Concrete Structures and Materials, 11 (2016) 17-28.
976 [76] Z. Makhloufi, E.H. Kadri, M. Bouhicha, A. Benaissa, Resistance of limestone
977 mortars with quaternary binders to sulfuric acid solution, Construction and Building
978 Materials, 26 (2012) 497-504.
979 [77] M.T. Bassuoni, M.L. Nehdi, Resistance of self-consolidating concrete to sulfuric
980 acid attack with consecutive pH reduction, Cement and Concrete Research, 37 (2007)
981 1070-1084.
982 [78] J. Monteny, A.B. E. Vincke, N. De Belie, L. Taerwe, D. Van Gemert, W. Verstraete,
983 Chemical, microbiological, and in situ test methods for biogenic sulfuric acid corrosion
984 of concrete, Cement and Concrete Research, 30 (2000) 623-634.
985 [79] H. Binici, O. Aksogan, Durability of concrete made with natural granular granite,
986 silica sand and powders of waste marble and basalt as fine aggregate, Journal of
987 Building Engineering, 19 (2018) 109-121.
988 [80] S. Ghorbani, I. Taji, J. de Brito, M. Negahban, S. Ghorbani, M. Tavakkolizadeh,
989 A. Davoodi, Mechanical and durability behaviour of concrete with granite waste dust
990 as partial cement replacement under adverse exposure conditions, Construction and
991 Building Materials, 194 (2019) 143-152.
992 [81] K. Aarthi, K. Arunachalam, Durability studies on fibre reinforced self compacting
993 concrete with sustainable wastes, Journal of Cleaner Production, 174 (2018) 247-255.
994 [82] J. Monteny, N. De Belie, L. Taerwe, Resistance of different types of concrete
995 mixtures to sulfuric acid, Materials and Structures, 36 (2003) 242-249.
996 [83] J.-X. Lu, Z.-H. Duan, C.S. Poon, Combined use of waste glass powder and cullet
997 in architectural mortar, Cement and Concrete Composites, 82 (2017) 34-44.
998 [84] H. Siad, M. Lachemi, M. Sahmaran, K.M.A. Hossain, Effect of glass powder on
999 sulfuric acid resistance of cementitious materials, Construction and Building Materials,
1000 113 (2016) 163-173.
1001 [85] C. Shi, J.A. Stegemann, Acid corrosion resistance of different cementing materials,
1002 Cement and Concrete Research, 30 (2000) 803–808.
1003 [86] K.V. Breugel, E.A.B. Koenders, Modelling of transport phenomena at cement
1004 matrix—Aggregate interfaces, Interface Science, 12 (2004) 423–431.
1005 [87] K.L. Scrivener, K.M. Nemati, The percolation of pore space in the cement

1006 pasteaggregate interfacial zone of concrete, Cement and Concrete Research, 26 (1996)
1007 35-40.
1008 [88] K.L. Scrivener, A.K. Crumbie, L. Peter, The interfacial transition zone (ITZ)
1009 between cement paste and aggregate in concrete, Interface Science 12 (2004) 411–421.
1010 [89] Tahir Celik, K. Marar, Effects of crushed stone dust on some properties of concrete,
1011 Cement and Concrete Research, 26 (1996) 1121-1130.
1012 [90] C. Perry, J.E. Gillott, The influence of mortar-aggregate bond strength on the
1013 behaviour of concrete in uniaxial compression, Cement and Concrete Research, 7 (1977)
1014 553-564.
1015 [91] P.J.M. Monteiro, J.C. Maso, J.P. Ollivier, The aggregate-mortar interface, Cement
1016 and Concrete Research, 15 (1985) 953-958.
1017 [92] C. Lian, Y. Zhuge, S. Beecham, The relationship between porosity and strength for
1018 porous concrete, Construction and Building Materials, 25 (2011) 4294-4298.

1019